Forest Ecology and Management 258 (2009) 1990–1999

Contents lists available at ScienceDirect

Forest Ecology and Management

journal homepage: www.elsevier.com/locate/foreco

Wildfire risk in the wildland–urban interface: A simulation study in northwestern Wisconsin

Avi Bar Massada [a,*], Volker C. Radeloff [a], Susan I. Stewart [b], Todd J. Hawbaker [c]

[a] Department of Forest and Wildlife Ecology, University of Wisconsin – Madison, 1630 Linden Drive, Madison, WI 53706, USA
[b] Northern Research Stations, U.S. Forest Service, 1033 University Avenue, Suite 360, Evanston, IL 60201, USA
[c] Rocky Mountain Geographic Science Center, U.S. Geological Survey, PO Box 25046, MS 516, Denver, CO 80225, USA

ARTICLE INFO

Article history:
Received 7 April 2009
Received in revised form 22 July 2009
Accepted 25 July 2009

Keywords:
Fire risk
Fire spread
FARSITE
MTT
Simulation modeling
WUI

ABSTRACT

The rapid growth of housing in and near the wildland–urban interface (WUI) increases wildfire risk to lives and structures. To reduce fire risk, it is necessary to identify WUI housing areas that are more susceptible to wildfire. This is challenging, because wildfire patterns depend on fire behavior and spread, which in turn depend on ignition locations, weather conditions, the spatial arrangement of fuels, and topography. The goal of our study was to assess wildfire risk to a 60,000 ha WUI area in northwestern Wisconsin while accounting for all of these factors. We conducted 6000 simulations with two dynamic fire models: Fire Area Simulator (FARSITE) and Minimum Travel Time (MTT) in order to map the spatial pattern of burn probabilities. Simulations were run under normal and extreme weather conditions to assess the effect of weather on fire spread, burn probability, and risk to structures. The resulting burn probability maps were intersected with maps of structure locations and land cover types. The simulations revealed clear hotspots of wildfire activity and a large range of wildfire risk to structures in the study area. As expected, the extreme weather conditions yielded higher burn probabilities over the entire landscape, as well as to different land cover classes and individual structures. Moreover, the spatial pattern of risk was significantly different between extreme and normal weather conditions. The results highlight the fact that extreme weather conditions not only produce higher fire risk than normal weather conditions, but also change the fine-scale locations of high risk areas in the landscape, which is of great importance for fire management in WUI areas. In addition, the choice of weather data may limit the potential for comparisons of risk maps for different areas and for extrapolating risk maps to future scenarios where weather conditions are unknown. Our approach to modeling wildfire risk to structures can aid fire risk reduction management activities by identifying areas with elevated wildfire risk and those most vulnerable under extreme weather conditions.

1. Introduction

Fire regimes of many ecosystems in the United States have been altered both by increasing numbers of human-caused ignitions (Syphard et al., 2008, 2007), and decades of fire suppression causing fuel accumulation (Hessburg and Agee, 2003; Agee, 1998). These two trends create management challenges, especially in areas where houses intermix or intermingle with natural vegetation, i.e., the wildland–urban interface (WUI) (Radeloff et al., 2005). Potentially high wildfire risk in the WUI raises the question of how to minimize wildfire risk to human lives and properties, and this requires knowledge about the current and future extent of the WUI, its socio-economical characteristics, and about likely fire patterns.

In 2000, the WUI area in the conterminous U.S. covered about 9% percent of the land area, and contained 39% of all houses (Radeloff et al., 2005). Housing growth in the U.S. is widespread, especially beyond the urban fringe (Haight et al., 2004; Radeloff et al., 2005), and these growth trends are likely to continue (Nowak and Walton, 2005). Future housing growth is predicted to increase the overall area of the WUI as well (Nowak and Walton, 2005; Theobald and Romme, 2007). Housing development also alters the fire size distribution in the vicinity of the WUI, and can directly and indirectly lead to increases in ignitions, but most fires are quickly extinguished and fire sizes remain small (Spyratos et al., 2007). The paradox of the WUI is that although more fires occur, they are generally smaller than backcountry wildfires due to early detection, intense suppression efforts and better firefighter accessibility. However, every ignition source has the potential to

* Corresponding author. Tel.: +1 608 263 4356; fax: +1 608 262 9922.
E-mail address: barmassada@wisc.edu (A. Bar Massada).

0378-1127/$ – see front matter
doi:10.1016/j.foreco.2009.07.051

grow into a large fire. Risk is influenced both by changing patterns of the landscape values at risk (i.e., homes) and the process generating the risk (ignitions and fire spread). The large and increasing number of lives and structures that are potentially exposed to wildfire hazard highlights the need to quantify wildfire risk in the WUI so that this risk can be minimized.

Finney (2005) defined fire risk as the combination of two main factors: [1] fire behavior distribution (e.g., flame lengths, energy release factors); and [2] fire effect, which is the expected net value change associated with a given fire behavior (Ager et al., 2006):

$$E[n] = \sum_{i=1}^{N}\sum_{j=1}^{n} p(F_i)[B_{i,j} - L_{i,j}] \tag{1}$$

where $E[n]$ is the expected net value change resulting from all N fire behaviors, $p(F_i)$ is the probability of an i fire behavior, and B_{ij} and L_{ij} are the jth values benefits and losses resulting from the ith fire behavior respectively (in principle, there could be benefits from fire). Fire effects represent the impact of fire on landscape values, such as damage to structures (e.g., houses and roads, which are more easily quantified), or change of habitat and ecosystem services (i.e., non-market values that are difficult to assess). Notice that this definition of fire risk differs from studies were fire risk is merely the chance that a fire might start (Hardy, 2005), and follows the definition by Bachmann and Allgower (2001). Similarly, Blanchi et al. (2002) defined fire risk as the combination of fire hazard, risk potential, and vulnerability. All fire risk assessment are different from fire danger assessments (e.g., San Miguel-Ayanz et al., 2003), such as the national fire danger rating system (Deeming et al., 1977), that summarize information about fire behavior and ignition risk at a regional scale using climate records and weather forecasts (Hessburg et al., 2007). Fire danger rating systems do not calculate explicit burn probabilities, and cannot assess the effects of potential fire events on landscape values.

The probability of a given fire behavior needs to account for fire spread which is largely dependent on spatio-temporal variation in ignitions, weather, topography, and fuels (Finney, 2005; Carmel et al., 2009). Burn probability maps should represent a wide range of ignition locations, weather conditions, and the resulting fire spread. This requires data for a large number of fires, based on many ignition locations and various weather conditions. In practice, it is impossible to obtain or simulate data for the infinite number of possible combinations of ignitions and weather conditions. Wildfire risk studies thus commonly focus on extreme weather conditions, since these favor the occurrence of large fire events that are harder to suppress, and pose the highest risk (Finney, 2005).

Empirical determination of fire risk requires information on an adequate number of fire occurrences for each weather condition, and an extensive suite of biophysical variables. In most places, these requirements (especially when fire records are scarce) limit the feasibility of an empirical approach (Brillinger et al., 2006; Wiitala, 1999). A solution is to use fire rotation times, which were used to assess the risk of stand replacing fires in the WUI in Northern lower Michigan (Haight et al., 2004). However, analyses using fire rotation data assume that future fire regimes will be similar to those of the past, and this may not be the case as landscapes become more settled and climate changes (Syphard et al., 2007; Lenihan et al., 2003). Additionally, empirical analyses use extensive spatial units over which fire histories are aggregated. These units may lack the spatial resolution needed to conduct fine-scale risk analyses, especially because fine-scale patterns of fire spread are difficult to account for with static statistical models. Another type of risk analysis is semi-probabilistic (or semi-empirical), in which historical fire data is complemented by field experiments or expert knowledge in order to introduce a mechanistic component into the empirical model (Blanchi et al., 2002).

Simulation modeling offers an alternative to empirical fire risk assessments since it does not require historical data, and rapidly rising computing power continues to expand its feasibility. Existing fire models can support simulations that provide detailed fire risk assessments, as shown in several recent studies. Several fire models have been used for fire risk assessments. BehavePlus (Andrews, 2007) is a non-spatial model that is used to gain better understanding of fire behavior, effects, and environment. FlamMap (Finney, 2006) adds the spatial component to BehavePlus, by calculating fire behavior separately for each pixel in the landscape, while using temporally constant weather conditions that are allowed to vary in space. Fire Area Simulator (FARSITE) (Finney, 1998) is a spatially explicit model that adds the temporal dimension to fire behavior, and allows for fire growth simulations. Minimum travel time (MTT) (Finney, 2002) is also a spatially explicit model that simulates fire spread across the landscape, but assumes temporally constant weather conditions. In Greece, spatially explicit fire risk was modeled as a function of socio-economic variables, biophysical factors, fuels, topography, and weather (Bonazountas et al., 2005), and resulted in five fire-related risk maps: [1] socioeconomic risk; [2] physical risk; [3] fire occurrence risk (equivalent to burn probability); [4] potential damage risk; and [5] integrated risk. In another analysis, areas with high fire potential and fire movement corridors were identified in a nature reserve in Brazil using FARSITE to simulate fire spread from four ignition points (Mistry and Berardi, 2005). FARSITE was also used to assess fire risk in Mt. Carmel, Israel using 600 random ignitions and randomly sampled weather and wind sequences, and results showed a good agreement between the spatial patterns of the simulated burn probabilities and actual fire records (Carmel et al., 2009). A similar approach was taken in a study that modeled wildfire risk to the habitat of an endangered owl species in Central Oregon (Ager et al., 2007). In that work, wildfire spread was simulated from 1000 random ignitions using MTT with constant weather conditions that corresponded to the conditions during an actual wildfire in that area. MTT also predicted burn probabilities around Missoula, Montana using 20,000 random fires, based on 98th percentile weather conditions (Finney, 2005), but the author cautioned that the resulting map has limited value for risk assessment, since MTT assumes constant weather conditions. To date, the simplifications necessary to conduct a robust wildfire risk assessment in WUI areas using spatially explicit fire simulation models precluded use of varying weather conditions.

The primary objective of this study was to assess wildfire risk to structures and land cover types in a WUI area in northwestern Wisconsin. The secondary objective was to explore how using extreme versus normal weather data in the models affected the predicted burn probability of the landscape and the wildfire risk to the structures in the WUI.

2. Methods

2.1. Study area

Our study was conducted in a 60,000 ha area west of Minong, northwestern Wisconsin, bordered by U.S. Highway 53 on the east, and the Namekagon and Saint Croix Rivers on the west (Fig. 1). We selected this area for our study because it is representative in terms of housing growth patterns for many areas in the rural U.S. Midwest, and since it is an area with comparatively high fire frequency.

Our study area is part of the northwestern Wisconsin Pine Barrens, a glacial outwash plain with very sandy soils. The topography is flat to gently rolling, with elevations ranging from

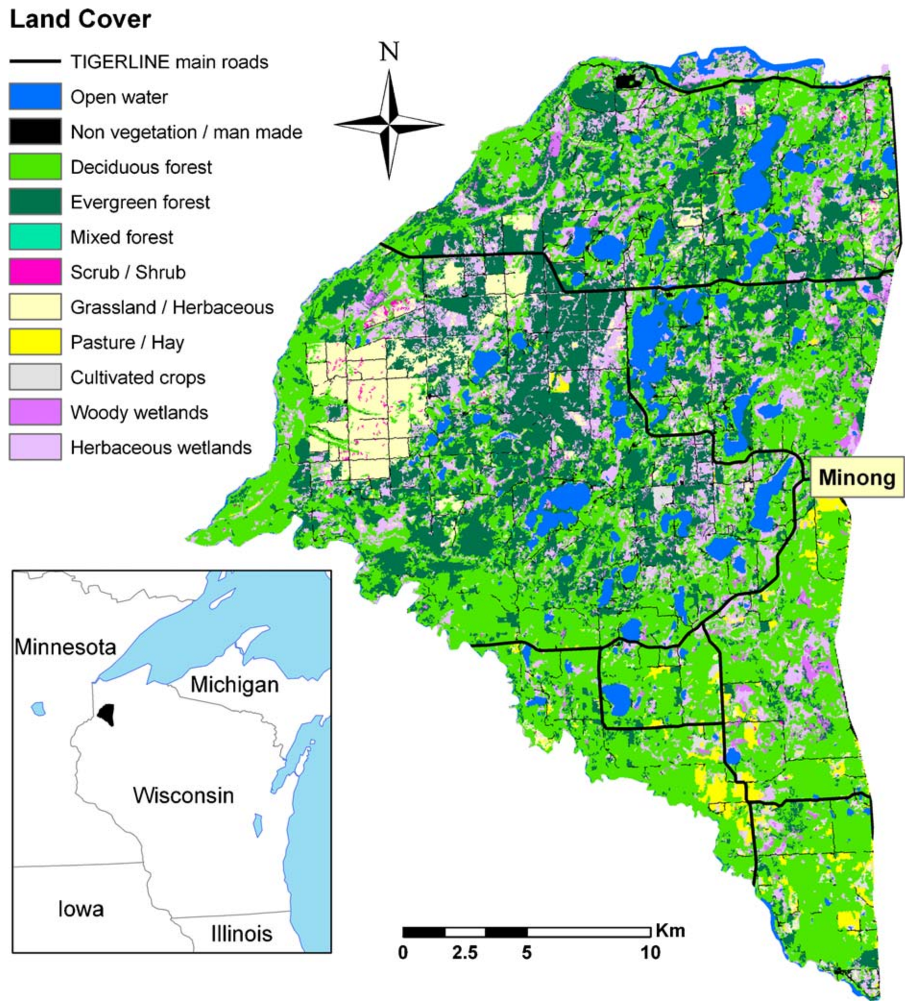

Fig. 1. Land cover map of the study area (derived from the 2001 National Land Cover Database), and the location of the study area in northwestern Wisconsin (black polygon).

270 to 400 m. The water table is high, and the study area contains many lakes. Climate is characterized by cold winters and short, mild summers. The mean January temperature and precipitation are −8.9 °C and 30.2 mm, respectively; and the mean August temperature and precipitation are 19 °C and 106.4 mm, respectively. The predominant wind direction is northeast, though wind directions vary over the year, and wind speeds are generally low (the average speed between 1998 and 2009 was 10.6 km/h). The northwestern Wisconsin Pine Barrens are more fire-prone than any other eco-region in the state (Radeloff et al., 2000). Historically, wildfires are most frequent in April, when the relative humidity is low and the vegetation is dry at the beginning of the growing season (Sturtevant and Cleland, 2007; Cardille and Ventura, 2001).

Vegetation is a mosaic of forests, clear cuts, and agricultural fields. The dominant tree species are jack pine (*Pinus banksiana* Lamb), accompanied by red and white pine (*Pinus resinosa* Ait. and *Pinus strobus* L., respectively); burr, red, and pin oak (*Quercus macrocarpa* Michx., *Quercus rubra* L., and *Quercus ellipsoidalis* E.J. Hill, respectively); and trembling aspen (*Populus tremuloides* Michx.) (Radeloff et al., 1999). According to the National Land Cover Data (NLCD, 2001), the major vegetated land cover types are deciduous forest (41%), evergreen forest (24%), herbaceous wetlands (14%), and grasslands (5%). Other, less common land cover types include woody wetlands, cultivated crops, scrublands, mixed forest, and pastures (Fig. 1).

Logging, which started in the mid-18th century, began a century of major land use changes (Radeloff et al., 1999). Logging slash provided fuel for many wildfires and until approximately 1930, logging, fires, and farm settlement opened the landscape and largely removed forest cover. In the 1930s, reforestation began and so did fire suppression. In recent decades, there has been an increase in housing development, mainly for recreational purposes, with the majority of new houses being built near lakes (Gonzales-Abraham et al., 2007a, 2007b). In many cases, houses are built amidst tall woody vegetation, consisting of pine and oak species. The majority of WUI in the study area is characterized as intermix, in which housing density is low and wildland vegetation cover is high (Radeloff et al., 2005).

2.2. Fire models

In order to assess fire risk, we used a dynamic modeling approach. We simulated wildfire spread and behavior with two commonly used models: FARSITE (Finney, 1998) and MTT (Finney, 2002), as implemented in FlamMap (Finney, 2006). FARSITE is a dynamic, spatially explicit fire model that uses the Huygens principle of wave propagation to determine the expansion of a polygonal fire front through time (Richards, 1990). FARSITE distinguishes between two fire behaviors and uses separate models for surface fires (Rothermel, 1972) and crown fires (Van Wagner, 1977). FARSITE requires a large set of input parameters to capture weather, fuels, and topographic elements. Weather data is supplied as streams of temporal data, consisting of minimum and maximum daily temperature and relative humidity (and their

Table 1
Description of fuel models in the study area.

Fuel model	Code	Description
91	NB1	Urban
93	NB3	Agriculture
98	NB8	Water
99	NB9	Barren
101	GR1	Grass is short naturally or after heavy grazing
103	GR3	Continuous, coarse humid climate grass, any shrubs do not affect fire spread
105	GR5	Humid climate grass, fuelbed depth about 2 feet
106	GR6	Continuous humid climate grass, not so coarse as GR5
108	GR8	Continuous coarse humid climate grass, spread rate and flame length may be extreme if grass is fully cured
122	GS2	Shrubs are 1–3 feet high, grass load is moderate, spread rate high and flame length moderate
123	GS3	Moderate grass/shrub load, depth is less than 2 feet, spread rate is high and flame length is moderate
142	SH2	Woody shrubs and shrub litter, fuelbed depth about a foot, no grass, spread rate and flame low
161	TU1	Low load of grass and/or shrub with litter, spread rate and flame low
162	TU2	Moderate litter load with some shrub, spread rate moderate and flame low
165	TU5	Heavy forest litter with shrub or small tree understory, spread rate and flame moderate
182	TL2	Broadleaf, hardwood litter, spread rate and flame low
183	TL3	Moderate load conifer litter, light load of coarse fuels, spread rate and flame low
186	TL6	Moderate load broadleaf litter, spread rate and flame moderate
201	SB1	Light dead and down activity fuel, fine fuel is 10–20 t/ac, 1–3 in. in diameter, depth less than 1 feet, spread rate moderate and flame low

corresponding time of day), daily precipitation, and hourly wind speed, direction, and cloud cover. Fuel data uses either the 13 Anderson fuel models (Anderson, 1982), the 40 Scott and Burgan fuel models (Scott and Burgan, 2005), or custom fuel models. Additional input data includes GIS raster layers of elevation, slope, aspect, canopy cover, crown height, crown base height, and crown bulk density. The user defines the ignition points and the length of the simulation. The model generates the following outputs: fire arrival time, fireline intensity, flame length, rate of spread, heat per unit area, reaction intensity, crown fire activity, and spread direction.

MTT (Finney, 2002) is a much faster algorithm than FARSITE and predicts fire behavior using constant weather conditions and wind directions for the duration of the fire. Here, we used MTT to speed up the analysis when constant weather conditions were used. MTT calculates the fastest fire travel times along straight lines connecting cells in a grid. Calculations are based on fire behavior models similar to the FARSITE surface fire module (Rothermel, 1972). MTT uses the same inputs as FARSITE, and the results of both models are practically interchangeable when weather conditions are constant (Finney, 2002). The assumption of constant weather conditions limits the feasibility of using MTT for simulating long fire events, but for shorter burn times, its results are acceptable (Finney, 2005).

We used FARSITE and MTT to simulate fire behavior following 6000 random ignitions across the study area (excluding water bodies). The duration of all fires was set to 12 h, since according to the Federal Wildland Fire Occurrence Data almost all fires in the region are suppressed within that period (http://wildfire.cr.usgs.gov/firehistory/data.html). The 6000 FARSITE simulations used normal weather sequences, described in detail below. For each fire, the model calculated the fireline intensity, rate of spread, spread direction, and fire perimeter. MTT simulations were split into 64 sets of multiple randomly ignited fires under extreme weather conditions (see Section 2.4), with the total number of fires being 6000. The large number of FARSITE simulations was carried out by automating the graphical user interface of FARSITE using HP QuickTest professional, a functional software testing program.

2.3. Input themes

The fuel and topography inputs required for both models were downloaded from LANDFIRE (http://www.landfire.gov/) at 30-m spatial resolution. The objective of the LANDFIRE project is to provide nationwide, landscape-scale geospatial products to support fire and fuels management planning (Rollins and Frame, 2006). LANDFIRE products include all of the spatial data required to run FARSITE and MTT, and are based on Landsat data, extensive field samples, and statistical modeling. We selected the 40-category fuel model map of Scott and Burgan (Table 1) for our study in order to increase ecological realism. After initial simulations, it became apparent that the representation of roads in the Scott and Burgan map was problematic, since many roads, including highways, were discontinuous, and this allowed fires to spread across these de facto firebreaks. We thus corrected road representation in the fuel map with US census bureau TIGERLINE road data downloaded from the Environmental Systems Research Institute (ESRI, http://www.esri.com/data/download/census2000_tigerline/index.html). The vector road data was integrated into the fuel map, and the road pixels were reclassified into one of the two fuel types. TIGERLINE road categories that represent primary and secondary roads, usually wider than 30 m (A21 and A31 in the study area) were classified as "urban" fuel type (NB1) and no surface fire could spread across these. All other roads were classified as short grass fuel type (GR1) that allows slow fire spread, since minor roads are typically narrower than 30 m (the pixel size of the fuel map) and may be partially vegetated (in the case of dirt roads). The original representation of roads in the LANDFIRE data would have artificially introduced fuel breaks, while allowing unconstrained fire spread in other areas where roads were discontinuous. Our approach is more conservative than the omission of roads from the fuel map, an alternative approach previously taken by LaCroix et al. (2006) that modeled the effect of landscape structure on wildland fire spread in the Chequamegon National Forest, to the East of our study area. However, classifying smaller roads as short grass fuel types maintains realism, in that this area's sandy soils and flat topography lend themselves to a proliferation of small, minimally-maintained two-tracks.

2.4. Weather data

We used two types of weather scenarios. Actual, hourly weather sequences were used for the FARSITE simulations, and 95th percentile constant weather data was used for the MTT simulations. Based on 15 years of historical fire data that included 13,513 fires (including ignition location, cause, duration, and size), Sturtevant and Cleland (2007) reported that the fire season in northern Wisconsin begins in March and ends in November, with

Table 2
The wind data used for the extreme weather MTT simulations.

	March	April	May	June	July	August	September	October	November
N	88	185	191	33	36	7	11	49	19
NE	121	1501	490	126	95	20	15	43	38
E	6	103	36	15	18	13	7	7	10
SE	0	0	24	0	3	2	0	0	0
S	39	41	191	50	18	21	30	10	3
SW	28	123	155	58	51	27	15	30	15
W	72	267	191	113	95	33	30	99	39
NW	110	226	167	58	63	23	24	119	53
Total (%)	463 (7.7)	2446 (40.8)	1446 (24.1)	454 (7.6)	378 (6.3)	147 (2.4)	133 (2.2)	356 (5.9)	178 (3)
Speed (km/h)	22.53	27.35	24.14	20.92	20.92	19.31	20.92	22.53	22.53

Values represent the number of times a given wind direction is used in a given month. The corresponding wind speed (constant per month) appears in the bottom row.

the majority of fires occurring in April (~40%). Additionally, there is considerable monthly variation in fire occurrence during the fire season. Accounting for that, we weighted our weather data according to the temporal distribution of fires and separated the 6000 ignitions into nine monthly subsets according to the fraction of fires in each month in the historical dataset (i.e., $N = 2446$ ignitions were assigned to April, since 40.8% of the actual fires occurred in April). For the FARSITE simulations, N normal weather sequences of 12 h were picked at random for each monthly subset. Hourly weather data that included temperature, relative humidity, wind speed and direction, and precipitation was obtained from a 10-year dataset (1999–2008) of hourly weather data collected at the Minong remote automated weather station (RAWS) at the eastern edge of our study area (http://www.raws.dri.edu/cgi-bin/rawMAIN.pl?sdWMNN).

For the MTT simulations, the 95th percentile temperatures and relative humidity for each month were calculated from the same weather dataset used for the FARSITE simulations. The weather data were used solely for fuel moisture calculation by MTT before the start of the simulations. Wind speed and direction have a large impact on fire spread in MTT, but they both vary considerably through time, even at a monthly scale. We thus split the MTT simulations into additional subsets according to wind directions. For each month, we calculated the 95th percentile wind speed. For that wind speed, we determined the frequency distribution of all major wind directions during that month (i.e., actual directions were binned into the eight major wind directions: N, NE, E, etc.). The possible total number of simulation subsets that could result from this process is 72 (nine months × eight wind directions). In our case, six subsets had no winds at the 95th percentile speed from the Southwest, so the actual number of subsets we used was 66 (Table 2).

2.5. Structure data

In the U.S., decennial housing data are available nationwide at the census block level. Census blocks are delineated by roads, waterways or political boundaries, and in urban areas they can be as small as a single block. However, the size of census blocks is highly variable, and in rural WUI areas like northern Wisconsin, the size of these blocks is relatively large, so that the spatial resolution of housing data is sometimes much coarser (few kilometers) than the resolution of the fire model outputs (30 m). We therefore assessed the risk to structures rather than by census blocks. We define structures as human-built objects that may be houses or non-housing buildings (e.g., commercial or agricultural buildings). Individual structures were digitized manually as points from 1-m resolution color aerial photographs from the summer of 2005 (National Agricultural Imagery Program), available at the National Map seamless server (http://seamless.usgs.gov/index.php). In places where structures appeared to be obstructed by overhead tree canopies, driveways and docks (near lakes) were used as indicators of the presence of structures (Gonzales-Abraham et al., 2007b). Overall, 3768 structures were mapped in the 600 km^2 study area.

2.6. Risk assessment

Two burn probability maps were constructed: one for the normal and one for the extreme weather scenarios, by summing the burn areas of all individual fires, and dividing the sum by the total number of ignitions (6000). The resulting map portrays the burn probability for each pixel given that there were 6000 random ignitions under normal weather conditions for the FARSITE simulations, and 6000 under extreme weather conditions for the MTT simulations. The structures map was overlaid on the burn probability maps, and for each structure the burn probability was derived from the burn probability map under the assumption that if a pixel containing a structure burned, the structure burned as well. In this manner, we identified structures with higher fire risk, though we simplified the risk term (Eq. (1)) by defining the loss term at the structure level, regardless of its actual economic value. We acknowledge that the actual ignition of a structure within a given fire perimeter will depend on other factors, such as building materials, defensible space, and so on (Cohen, 2000), but we had neither housing data that could capture these factors nor the empirical data to model the ignition probabilities as a function of these factors.

We also assessed fire risk in relation to different land cover types and used the 2001 National Land Cover Data (NLCD) to determine land cover in the study area. The NLCD cover classes differ from the fuel maps that were used for the fire simulations, since fuel models account also for the vertical structure of vegetation and the existence of understory vegetation which is not captured by the broader NLCD classes. In addition, LANDFIRE data was developed using different algorithms than the NLCD, though NLCD was used to validate some aspects of LANDFIRE. The land cover map was overlaid on the burn probability maps, and for each land cover class we calculated the distribution of burn probabilities. The four NLCD classes that correspond to non-vegetated areas and extensive human development (open space, low intensity, medium intensity, and high intensity development) tended to overlap with road and non-fuel areas, and were therefore omitted from the analysis.

The effect of different types of weather data (extreme versus normal) on fire risk were assessed by comparing the distributions of risk levels (number of burns per structure and burn probability by cover class) and the spatial configuration of burn probabilities. In addition, fire risk to structures was calculated for the entire study area using Eq. (1). Since we examined only a single fire behavior (burned/unburned), and fires provided just losses, the equation was modified as follows:

$$E[n] = \sum_{j=1}^{n} p(F) L_j \tag{2}$$

Fire risk (E) was therefore calculated as a linear combination of burn probabilities and their corresponding number of structures.

3. Results

3.1. Fire patterns under normal weather conditions

Simulated fires under normal weather conditions were small, with a mean fire size of 11.76 ha. The largest fire occurred in April, covering an area of 253 ha in the western part of the study area. The mean area of fires varied between months, with the spring fires (March–May) being generally larger than fires in the subsequent months (Fig. 2). The largest mean fire size occurred in March, after which fire areas decreased continuously until September. During the autumn months, mean fire size increased after the lowest fire size in September, and peaked in November, though this peak was lower than the average size of the spring fires.

The frequency distribution of all fires showed that the majority of fires (54.7%) were smaller than 10 ha (Fig. 3). Only a small proportion of fires (28 out of 6000) were larger than 100 ha. The pattern of fire size distribution is similar to that found in other studies (Ager et al., 2007) and to the actual fire size distribution in northern Wisconsin according to the Federal Wildland Fire Occurrence Data (http://wildfire.cr.usgs.gov/firehistory/data.html).

The size and the date of individual fires could only be summarized for the FARSITE normal weather simulations. The MTT algorithm implemented in FlamMap calculates burn probabilities for multiple fires with random ignition locations directly, without providing individual fire characteristics. Therefore, we could not compare the fire size distribution from the MTT simulations to the FARSITE fire size distribution.

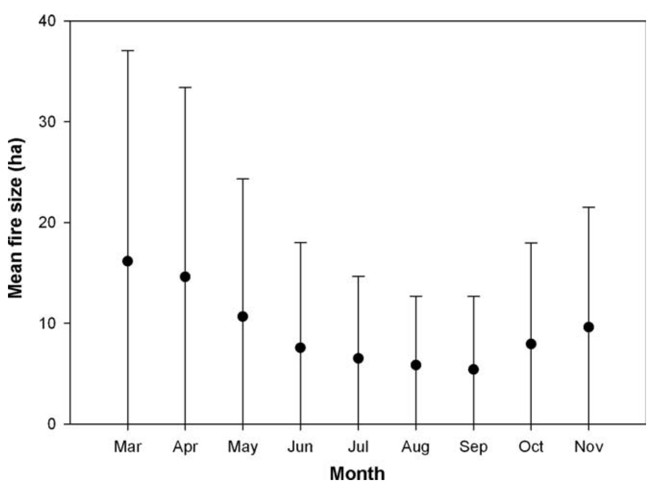

Fig. 2. Mean fire size per month in 6000 FARSITE simulations under normal weather conditions. Error bars represent standard deviation.

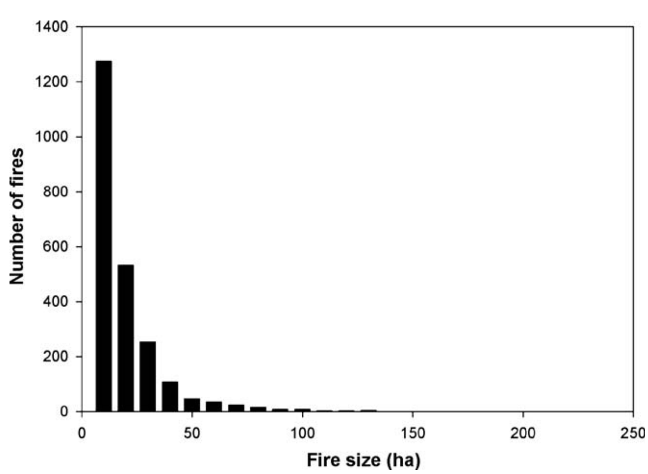

Fig. 3. Size distribution of the 6000 FARSITE simulations under normal weather conditions.

3.2. Burn probabilities

The burn probability maps show a clear spatial trend (Fig. 4). In both models (and thus for both normal and 95th percentile weather conditions), the ‘hotspot’ with the highest burn probabilities across the largest area was in the western part of the study area. This hotspot corresponded to a large open area with continuous humid grassland (fuel type GR3). The southeastern portion of the study area had much lower burn probabilities under both weather conditions. This area contains greater proportions of deciduous forests and agricultural fields.

Under extreme weather conditions, burn probability for any pixel in the study area ranged from 0% to 0.37%, compared to 0% to 0.26% for the normal weather conditions. 84.56% of the terrestrial area burned at least once under the extreme weather conditions, compared to 62.87% under the normal conditions (Fig. 4). The Spearman correlation between the two burn probability maps was 0.63 ($P < 0.01$).

3.3. Risk to structures

The overall risk to structures (Eq. (2)) was 1.07 and 0.48 for the extreme and normal weather conditions, respectively. Under the extreme conditions, 73% of the structures burned in at least one simulation, and many structures burned in several simulations (Fig. 5). In contrast, only 47% of the structures burned at least once under the normal weather conditions. There were no structures in the highest burn probability areas (e.g., in the hotspots), and the maximal burn probability for any single pixel that contained a structure (0.18% under extreme weather conditions) was less than half of the maximum burn probability in the entire study area (0.37%). The burn probabilities of structures under normal weather conditions explained only a small portion of the variation of the corresponding burn probabilities under extreme weather conditions (Fig. 6), although the regression was significant ($R^2 = 0.055$, $P < 0.001$). The root mean square error between the burn probabilities of structures under normal and extreme weather was 0.032 (in percent, which corresponds to an RMSE of 1.93 fires for burn events). The burn probabilities of the structures differed significantly between simulations using different weather conditions (Kolmogorov–Smirnov test, $D = 0.28$, $P < 0.001$).

3.4. Fire risk and WUI land cover

Different land cover classes exhibited varying burn probabilities and these differences were generally consistent under both weather conditions (Figs. 7 and 8). Extreme weather conditions generated higher burn probabilities for all land cover classes, when compared to normal weather conditions. Under extreme weather conditions, the highest average burn probability occurred in the grasslands/herbaceous vegetation class, which is concentrated in a wildlife management area in the western part of the study area. Lower burn probabilities were observed in scrub/shrubs, evergreen

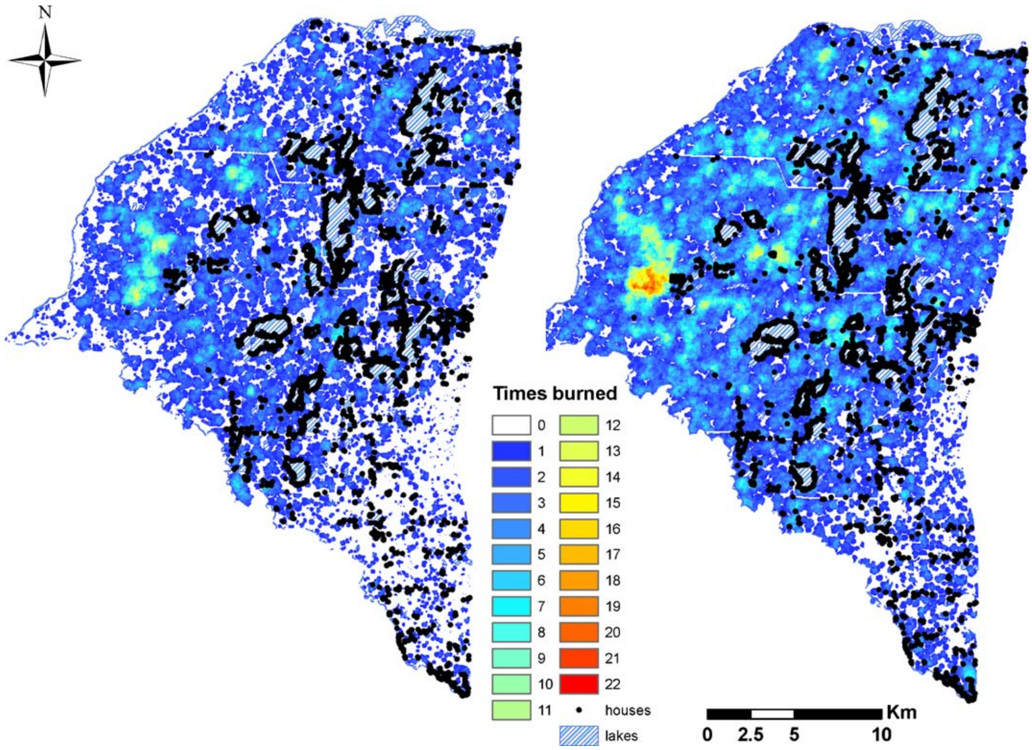

Fig. 4. Simulated fire occurrence under normal weather conditions (using FARSITE, left) and extreme weather conditions (using MTT, right) based on 6000 random ignition locations.

forests, mixed forests, emergent herbaceous wetlands, and deciduous forests (in this order). Cultivated crops and pasture/hay had the lowest average burn probabilities. Under the normal weather conditions, cultivated crops had a somewhat higher burn probability, compared to its relative burn probability under the extreme conditions. On the other hand, herbaceous wetlands had a comparatively lower burn probability.

4. Discussion

We assessed wildfire risk to structures in a WUI area in northwestern Wisconsin using fire simulation models. As expected, fire risk to structures varied substantially in space, and between weather conditions, even when ignition locations were random. Although normal and extreme weather conditions yielded generally similar spatial patterns of burn probability, the fine-scale differences of fire risk (i.e., at the level of a structure) were significantly different between normal and extreme weather conditions.

In WUI areas, wildfires pose a risk to human lives and property, highlighting the necessity for thorough risk analyses to aid management activities (GAO, 1999). Yet, federal land management agencies in the US have lacked wildfire risk analysis tools for years (GAO, 2004). The method presented in this study might serve as a supplementary tool that can aid management decisions in fire-prone WUI areas, provided that the necessary data (weather, fuels, and housing) are available. Building on prior studies (Finney, 2005; Carmel et al., 2009; Ager et al., 2007), but taking them a step further, we assessed fire risk using multiple simulations (6000) of dynamic fire models under varying weather conditions and ignition locations. The main strength of a multiple-simulation approach is the potential to account simultaneously for the effects of different factors that affect fire spread (i.e., weather, wind, and ignitions). In the case of weather and wind, these factors can either be based on actual data, or represent extreme cases, or examine hypothetical conditions (such as the impact of climate change on fire behavior) that may be assessed using future weather predictions from models (Keane et al., 2008).

Fuel distribution has a large influence on fire spread in FARSITE and MTT (and other fire models as well). Development of accurate fuel maps that cover wide geographical extents has been a major research task for many decades (Keane et al., 2001), and this information is now available through the LANDFIRE project (Rollins and Frame, 2006) for the entire United States. The LANDFIRE data are the best available data for large-scale fire simulations, and the only data that are readily available to managers, but the information is not without problems. Inaccurate mapping of burnable fuel types, which affects mainly the rate of fire spread and its behavior and characteristics, is one issue; the second is inconsistent mapping of unburnable surfaces (e.g., roads and lakes). This can have large impacts on the spatial pattern of fire spread, since the non-burnable surfaces act essentially as fire-breaks. In initial tests, the inconsistent representation of the roads in the fuel map we used lead to anomalies in fire spread. To overcome this, we used TIGERLINE road data and recommend that other analysts consider a similar approach when using fuel maps from the LANDFIRE project for fire simulation on landscapes with roads.

An additional input theme, ignition locations, may have a large impact on the spatial pattern of fires. Burn probability maps are often created using random ignition locations (Finney, 2005; Ager et al., 2007; this study), but actual ignition locations are not random. Ignition probabilities are generally higher near roads, railroad tracks, power lines, and other areas of human activities (Syphard et al., 2008; Sturtevant and Cleland, 2007; Vasconcelos et al., 2001; Cardille and Ventura, 2001). However, ignition probability modeling is not well developed and models do not seem to generalize; they vary between areas, and may depend on weather conditions, fuels, and the exact type of human activity. Using inappropriate ignition patterns may bias the outcomes of any spatial fire model, and introduce errors of unknown source, magnitude and effect into fire risk assessment. And since we

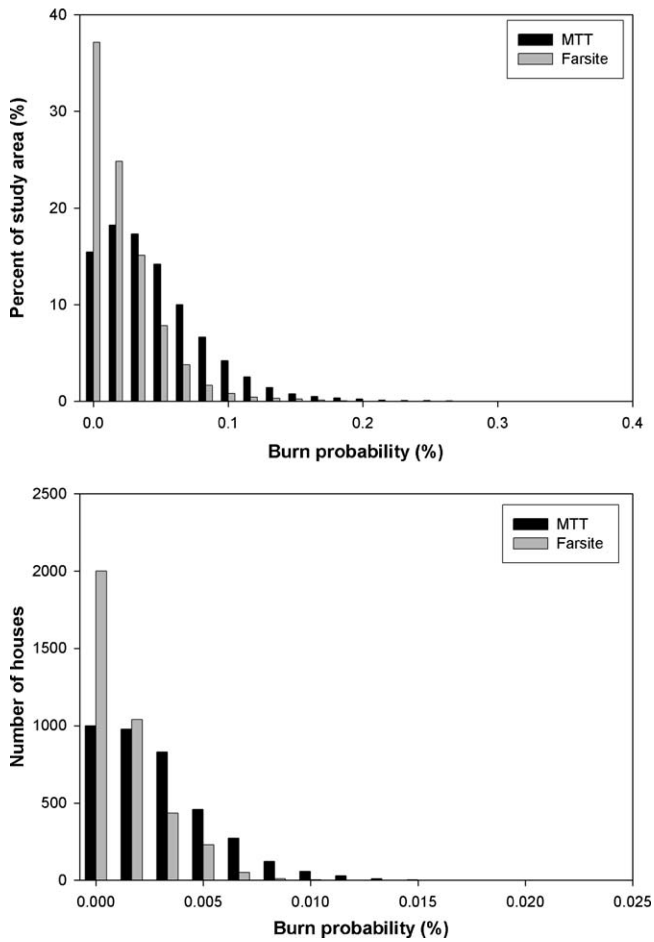

Fig. 5. Distributions of burn probabilities across the study area (*top*), and for structures (*bottom*). Extreme (MTT) and normal (FARSITE) weather conditions are shown in black and gray, respectively.

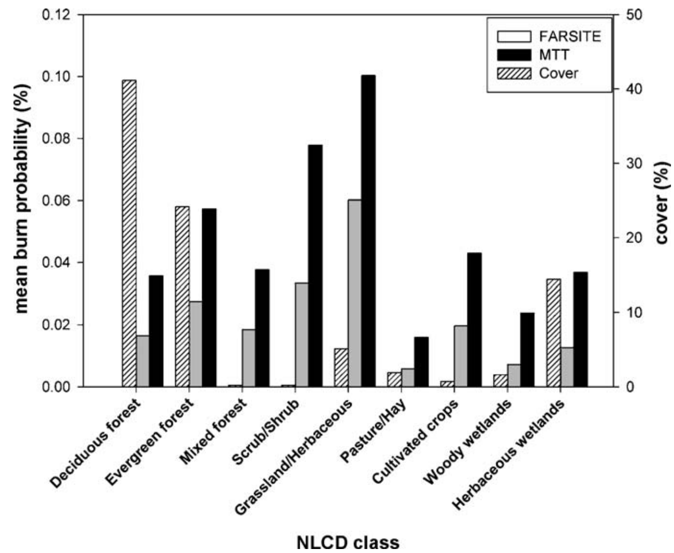

Fig. 7. The percent cover of vegetated land cover classes (*diagonal stripes*) and their mean burn probability under normal (*gray*) and extreme (*black*) weather conditions.

expect more ignitions to occur in the WUI, the risk assessment might be highly sensitive to the parameters of the ignition model (i.e., a small change in the ignition model may result in a large change in fire risk). The only fire start model that contains our study area (Sturtevant and Cleland, 2007) had a resolution too low for our needs (2.6 km^2 grid cells rather than point locations). In the absence of a suitable ignition probability model parameterized for our study area, we used a random ignition model to normalize the effect of ignition locations. Our choice of a random ignition model also enables future comparisons with similar studies in other locales, especially where the ignition patterns are unknown (which is common due to insufficient empirical fire data). However, it would be interesting to examine the difference in fire risk resulting from models based on random ignitions versus a suitable ignition model, or empirical ignition data.

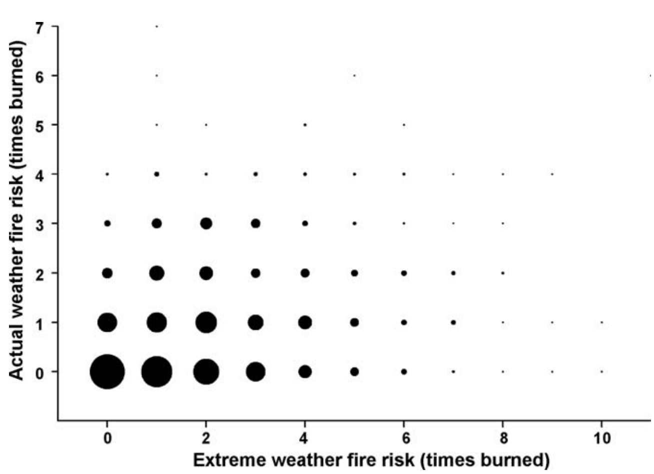

Fig. 6. The relation between the number of times structures burn under normal (FARSITE) and extreme (MTT) weather conditions following 6000 random ignitions in the study area. Dot size is proportional to the number of occurrences.

The choice of weather conditions had a significant effect on the results of our fire models and consequently on the risk assessment. It is not surprising that extreme weather posed a higher wildfire risk than average weather. What we have shown here is that the spatial pattern of risk (i.e., which structures are at higher risk or which areas are more fire-prone) may also change, and these changes can be quantified. Therefore, risk maps that are based on extreme weather condition should be interpreted with care if they are used for actual fire and fuel management, since they do not necessarily reflect the most realistic spatial pattern of risk. Furthermore, comparisons of risk maps from different areas need to take into account the pronounced effect of weather conditions. For example, the range of burn probabilities that were obtained for the 95th percentile weather conditions were an order of magnitude lower that those reported by Finney (2005) for the landscape around Missoula, Montana under 98th percentile weather conditions and constant wind speed and direction.

In our study area, fire risk to structures over the entire analysis extent was twice as great under extreme weather conditions as for the normal weather conditions. In addition, much larger proportions of the study area and of structures were burned under the extreme conditions. Even though these differences were expected between such different weather scenarios, we were surprised by the only moderate correlation between the burn probability maps. We had expected that normal weather conditions would simply result in uniformly lower burn probabilities. As expected, land cover classes exhibited different fire risks. The fire risk of different land cover types is affected by the biophysical properties of their corresponding fuel types, but also by the interaction between ignition locations, weather conditions, and the spatial patterns of different land cover types. Grasslands had the highest burn probability, twice as high as the forest type with the highest burn probability, evergreen forests. The majority of grasslands are located in a wildlife management area in the western part of the

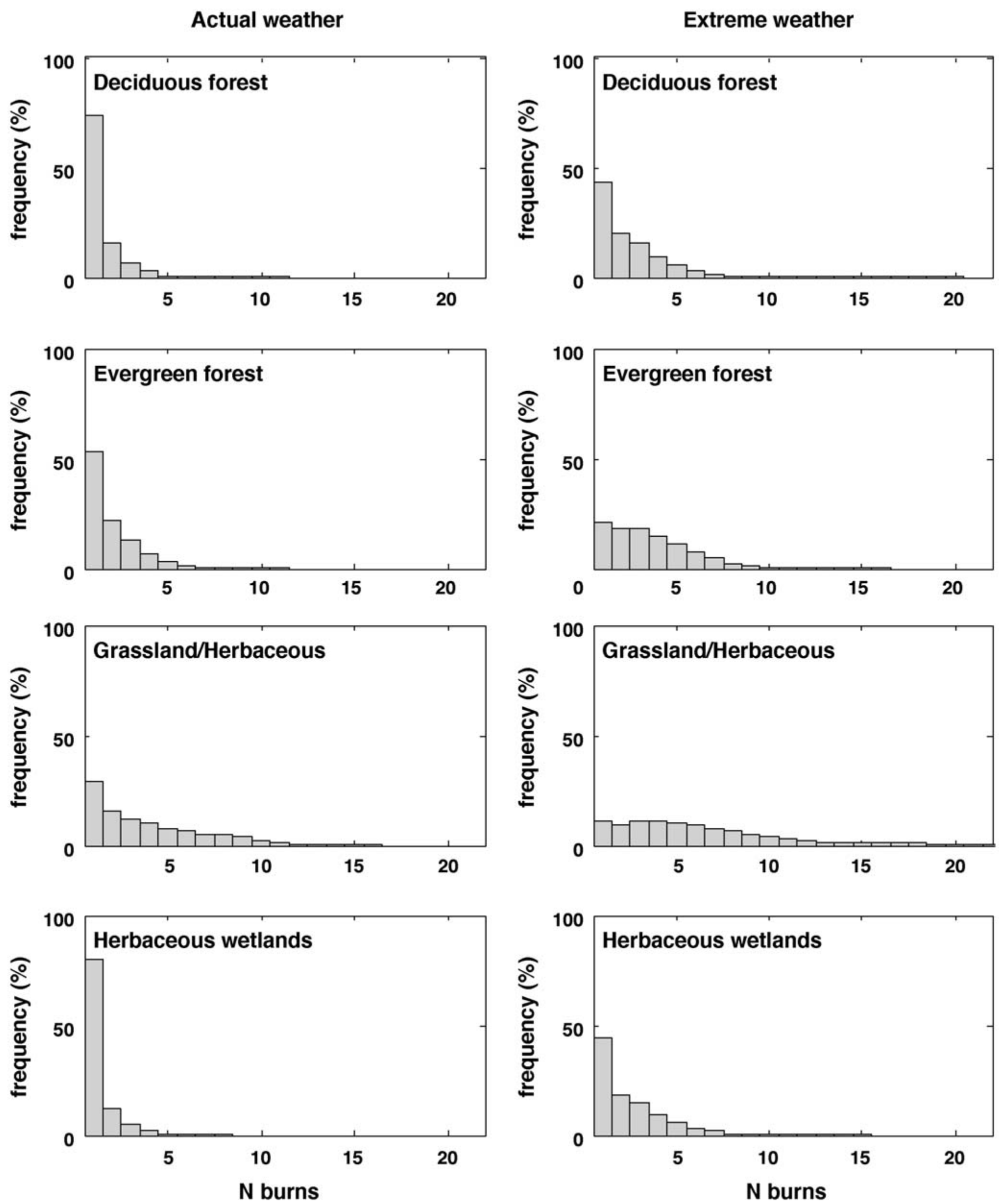

Fig. 8. The distribution of number of fires (out of 6000 random ignitions) under normal (*left column*) and extreme (*right column*) weather conditions for the four dominant vegetated land cover classes. Each bar represents a single burn probability, and its height depicts the percentage of pixels out of all pixels for the corresponding land cover class.

study area, where large and continuous grasslands allow rapid wildfire spread. Though there are no houses or other structures in the immediate vicinity of that fire hotspot, it may be desirable to manage the fuels in this area to prevent fire spread and smoke impacts to surrounding roads and communities.

The following management recommendations emerge from our analysis: [1] it is crucial to obtain the best available fuel maps prior to estimating fire risk. If LANDFIRE data is used, TIGERLINE road data should be used to correct the misrepresentation of roads in the fuel map; [2] Weather data should account for several types of conditions (versus just extreme weather), preferably normal fire season weather and extreme conditions weather, to represent both sides of the spectrum of fire behavior (e.g., Cheyette et al., 2008); and [3] a random ignition model should be used only in cases where there is an insufficient fire record to support the development of an empirical ignition model (e.g., Syphard et al., 2008).

Despite the minor limitations of the LANDFIRE data, and the FARSITE and MTT fire models, our results demonstrate that fire risk assessments for large areas are feasible, and provide important information for land managers. Due to the availability of LANDFIRE products and RAWS weather data, it is possible to replicate this approach in any place in the conterminous U.S., assuming that structure data is obtained by manual digitization from high resolution aerial imagery. While our study area represents mainly WUI conditions typical for the northern Great Lakes region, which is characterized by the abundance of lakes and a relatively flat topography, our approach is general enough to be applied to any WUI area. In WUI areas where topography plays a bigger role in fire spread, the spatial heterogeneity of fire risk is expected to be more pronounced (e.g., in the southern California mountainous WUI where fire spreads mainly along canyons, which often contain many structures, producing an extreme fire hotspot). Without fire risk assessments, fuel management and other fire prevention efforts are likely to be less effective. Our results also highlight that patterns of risk vary depending on normal or extreme weather conditions and that both types of risk patterns should preferably be accounted for in risk assessments. We conclude that dynamic fire models are a promising tool for more robust wildfire risk assessments, and that further research is warranted to validate and enhance the quality of data sources that are used in these models, and to develop realistic models of fire ignition locations.

Acknowledgments

We gratefully acknowledge support for this research by the U.S. Forest Service Northern Research Station. This manuscript benefited greatly from comments by J. Briggs, D. Hester, and two anonymous reviewers. References to HP and ESRI software products are provided for information only and do not constitute endorsement by the U.S. Geological Survey, U.S. Departments of Interior or Agriculture, or the U.S. Government, as to their suitability, content, usefulness, functioning, completeness, or accuracy.

References

Agee, J.K., 1998. The landscape ecology of western forest fire regimes. Northwest Science 72, 24–34.

Ager, A.A., Finney, M.A., McMahan, A., 2006. A wildfire risk modeling system for evaluating landscape fuel treatment strategies. In: Andrews, P.L., Butler, B.W. (Eds.), Fuels Management—How to Measure Success: Conference Proceedings, March 28-30, Portland, OR. USDA Forest Service, Rocky Mountain Research Station Proceedings RMRS-P-41, pp. 149–162.

Ager, A.A., Finney, M.A., Kerns, B.K., Maffei, H., 2007. Modeling wildfire risk to northern spotted owl (strix occidentalis caurina) habitat in Central Oregon, USA. Forest Ecology and Management 246, 45–56.

Anderson, H.E., 1982. Aids to Determining Fuel Models for Estimating Fire Behavior. USDA Forest Service, Intermountain Forest and Range Experiment Station, General Technical Report INT-GTR-122.

Andrews, P.L., 2007. BehavePlus fire modeling system: past, present, and future. In: Proceedings of 7th Symphosium on Fire and Forest Meteorological Society. October 23-25, Bar Harbor, Maine Available at:http://ams.confex.com/ams/pdfpapers/126669.pdf.

Bachmann, A., Allgower, B., 2001. A consistent wildland fire risk terminology is needed! Fire Management Today 61, 28–33.

Blanchi, R., Jappiot, M., Alexandrian, D., 2002. Forest fire risk assessment and cartograhpy—a methodological approach. In: Proceedings of IV International Conference on Forest Fire Research, November 18-23, Luso, Portugal.

Bonazountas, M., Kallidromitou, D., Kassomenos, P.A., Passas, N., 2005. Forest fire risk analysis. Human and Ecological Risk Assessment 11, 617–626.

Brillinger, D.R., Preisler, H.K., Benoit, J.W., 2006. Probablistic risk assessment for wildfires. Environmetrics 17, 623–633.

Cardille, J.A., Ventura, S.J., 2001. Occurrence of wildfire in the northern Great Lakes Region: effects of land cover and land ownership assessed at multiple scales. International Journal of Wildland Fire 10, 145–154.

Carmel, Y., Paz, S., Jahashan, F., Shoshany, M., 2009. Assessing fire risk using Monte Carlo simulations of fire spread. Forest Ecology and Management 257, 370–377.

Cheyette, D., Rupp, T.S., Rodman, S., 2008. Developing fire behavior fuel models for the wildland–urban interface in Anchorage, Alaska. Western Journal of Applied Forestry 23, 149–155.

Cohen, J., 2000. Preventing disaster: home ignitability in the wildland–urban interface. Journal of Forestry 98, 15–21.

Deeming, J.E., Burgan, R.E., Cohen, J.D., 1977. The National Fire-Danger Rating System—1978. USDA Forest Service, Intermountain Forest and Range Experiment Station, Ogden, UT, General Technical Report GTR-INT-39.

Finney, M.A., 2006. An overview of FlamMap fire modeling capabilities. In: Andrews, P.L., Butler, B.W. (Eds.), Fuels Management—How to Measure Success: Conference Proceedings, March 28–30, Portland. USDA Forest Service, Rocky Mountain Research Station Proceedings RMRS-P-41, pp. 213–220.

Finney, M.A., 2005. The challenge of quantitative risk analysis for wildland fire. Forest Ecology and Management 211, 97–108.

Finney, M.A., 2002. Fire growth using minimum travel time methods. Canadian Journal of Forest Research 32, 1420–1424.

Finney, M.A., 1998. FARSITE: Fire Area Simulator—Model Development and Evaluation. USDA Forest Service, Rocky Mountain Forest and Range Experiment Station, General Technical Report RP-4.

GAO, 2004. Wildland fires: forest service and BLM need better information and a systematic approach for assessing the risks of environmental effects. Washington, DC, GAO-04-705.

GAO, 1999. Western national forests: a cohesive strategy is needed to address catastrophic wildfire risk. Washington, DC, GAO/RCED-99-65.

Gonzales-Abraham, C.E., Radeloff, V.C., Hammer, R.B., Hawbaker, T.J., Stewart, S.I., Clayton, M.K., 2007a. Building patterns and landscape fragmentation in northern Wisconsin, USA. Landscape Ecology 22, 217–230.

Gonzales-Abraham, C.E., Radeloff, V.C., Hawbaker, T.J., Hammer, R.B., Stewart, S.I., Clayton, M.K., 2007b. Patterns of houses and habitat loss from 1937 to 1999 in northern Wisconsin, USA. Ecological Applications 17, 211–223.

Haight, R.G., Cleland, D.T., Hammer, R.B., Radeloff, V.C., Rupp, T.S., 2004. Assessing fire risk in the wildland–urban interface. Journal of Forestry 102, 41–48.

Hardy, C.C., 2005. Wildland fire hazard and risk: problems, definition, and context. Forest Ecology and Management 211, 73–82.

Hessburg, P.F., Agee, J.K., 2003. An environmental narrative of Inland Northwest United States forests, 1800–2000. Forest Ecology and Management 178, 23–59.

Hessburg, P.F., Reynolds, K.M., Keane, R.E., James, K.M., Salter, R.B., 2007. Evaluating wildland fire danger and prioritizing vegetation and fuels treatments. Forest Ecology and Management 247, 1–17.

Keane, R.E., Burgan, R.E., van Wagtendonk, J.W., 2001. Mapping wildland fuels for fire management across multiple scales: integrating remote sensing, GIS, and biophysical modeling. International Journal of Wildland Fire 10, 301–319.

Keane, R.E., Holsinger, L.M., Parsons, R.A., Gray, K., 2008. Climate change effects on historical range and variability of two large landscapes in western Montana, USA. Forest Ecology and Management 254, 375–389.

LaCroix, J.J., Ryu, S., Zheng, D., Chen, J., 2006. Simulating fire spread with landscape management scenarios. Forest Science 52, 522–529.

Lenihan, J.M., Drapek, R., Bachelet, D., Neilson, R.P., 2003. Climate change effects on vegetation distribution, carbon, and fire in California. Ecological Applications 13, 1667–1681.

Mistry, J., Berardi, A., 2005. Assessing fire potential in a Brazilian savanna nature reserve. Biotropica 37, 439–451.

Nowak, D.J., Walton, J.T., 2005. Projected urban growth (2000–2050) and its estimated impact on the US forest resource. Journal of Forestry 103, 383–389.

Radeloff, V.C., Mladenoff, D.J., Boyce, M.S., 2000. A historical perspective and future outlook on landscape scale restoration in the northwest Wisconsin Pine Barrens. Restoration Ecology 8, 119–126.

Radeloff, V.C., Mladenoff, D.J., He, H.S., Boyce, M.S., 1999. Forest landscape change in the northwestern Wisconsin Pine Barrens from pre-European settlement to the present. Canadian Journal of Forest Research 29, 1649–1659.

Radeloff, V.C., Hammer, R.B., Stewart, S.I., Fried, J.S., Holcomb, S.S., McKeefry, A.J., 2005. The wildland–urban interface in the United States. Ecological Applications 15, 799–805.

Richards, G.D., 1990. An elliptical growth model of forest fire fronts and its numerical solutions. International Journal for Numerical Methods in Engineering 30, 1163–1179.

Rollins, M.G., Frame, C.K., 2006. The LANDFIRE Prototype Project: Nationally Consistent and Locally Relevant Geospatial Data for Wildland Fire Management. USDA Forest Service, Rocky Mountain Research Station, Fort Collins, CO, General Technical Report RMRS-GTR-175.

Rothermel, R.C., 1972. A mathematical model for predicting fire spread in wildland fuels. USDA Forest Service Research Paper p. INT-115.

San Miguel-Ayanz, J., Carlson, J.D., Alexander, M., Tolhurst, K., Morgan, G., Sneeuwjagt, R., Dudley, M., 2003. Current methods to assess fire danger potential. In: Chuvieco, E. (Ed.), Wildland Fire Danger Estimation and Mapping: the Role of Remote Sensing Data. World Scientific Publishing, Singapore, pp. 21–61.

Scott, J.H., Burgan, R.E., 2005. Standard Fire Behavior Fuel Models: A Comprehensive Set for Use with Rothermel's Surface Fire Spread Model. USDA Forest Service, Rocky Mountain Research Station, General Technical Report RMRS-153.

Spyratos, V., Bourgeron, P.S., Ghil, M., 2007. Development at the wildland–urban interface and the mitigation of forest-fire risk. Proceedings of the National Academy of Sciences 104, 14272–14276.

Sturtevant, B.R., Cleland, D.T., 2007. Human and biophysical factors influencing modern fire disturbance in northern Wisconsin. International Journal of Wildland Fire 16, 398–413.

Syphard, A.D., Radeloff, V.C., Keuler, N.S., Taylor, R.S., Hawbaker, T.J., Stewart, S.I., Clayton, M.K., 2008. Predicting spatial patterns of fire on a southern California landscape. International Journal of Wildland Fire 17, 602–613.

Syphard, A.D., Radeloff, V.C., Keely, J.E., Hawbaker, T.J., Clayton, M.K., Stewart, S.I., Hammer, R.B., 2007. Human influence on California fire regimes. Ecological Applications 17, 1388–1402.

Theobald, D.M., Romme, W.H., 2007. Expansion of the US wildland–urban interface. Landscape and Urban Planning 83, 340–354.

Vasconcelos, M.J.P., Silva, S., Tomé, M., Alvim, M., Pereira, J.M.C., 2001. Spatial prediction of fire ignition probabilities: comparing logistic regression and neural networks. Photogrammetric Engineering and Remote Sensing 67, 73–83.

Van Wagner, C.E., 1977. Conditions for the start and spread of crown fire. Canadian Journal of Forest Research 7, 23–34.

Wiitala, M.R., 1999. Assessing the risk of cumulative burned acreage using the Poisson probability model. In: Gonzales-Caban, A., Omi, P.N. (Eds.), Proceedings of the Symposium on Fire Economics, Planning, and Policy; Bottom Lines. USDA Forest Service, General Technical Report PSW-GTR-173.